Korean J. Chem. Eng., **24**(5), 742-748 (2007)

Photobiocatalytic hydrogen production in a photoelectrochemical cell

Jaekyung Yoon and Hyunku Joo†

Greenhouse Gas Research Center, Fossil Energy & Environment Research Department, Korea Institute of Energy Research, 71-2 Jang-dong, Yusong-gu, Daejeon 305-343, Korea
(*Received 26 September 2006 • accepted 6 February 2007*)

Abstract−In this study the photobiocatalytic hydrogen production system was photoelectrochemically examined. Preliminary experiments with a mixed slurry system revealed the following five facts: direct, inter-phase, electron transfer from photocatalyst to enzyme in the absence of electron relay was a rate-determining step; the enzyme was deactivated by irradiated light (half after 10 days); physical properties (crystallinity, specific surface area, pore volume and radius) of the photocatalysts, obtained by two preparation methods (sol-gel and hydrothermal), were seldom correlated with the production rate; chemical properties were postulated to have been affected; and each material needed different reaction conditions such as pH and temperature. For the later salt-bridged system, the I-V relation for each prepared photocatalyst was measured (V_{fb} in the range of ca. −0.9~−1.0 and V_{oc} close to −1.1 V vs. Ag/AgCl in saturated KCl). The change in the amount of evolved hydrogen was also independently checked according to external bias (critical bias around 1.0 V). Then both reaction components were connected through a salt bridge to initiate light-induced hydrogen production for the hybrid system. The H_2 production exhibited an exponential trend and the Tris-HCl buffer showed the highest rate. A feasible reaction pathway was proposed.

Key words: Photocatalyst, Photobiocatalytic, Hydrogenase, Hydrogen, Factorial Design

INTRODUCTION

Environmental remediation using photocatalysts has been a major focus in many countries over the last decade. Numerous studies have focused on hydrogen evolution from water as a clean energy resource since the invention of photochemical water splitting over TiO_2 electrode. However, the photocatalytic process has been simultaneously criticized as being uneconomical compared to other oxidative treatment systems and up-to-date hydrogen production systems due to its inherently low efficiency and limitations resulting from the necessity for an appropriate light source and immobilization, which may increase the overall energy costs [1]. Therefore, research attention has focused on developing economically feasible photocatalytic systems with future commercial applications.

As far as photo-production of hydrogen is concerned, one of the IEA hydrogen programs (known as the Hydrogen Implementing Agreement (HIA)), Annex-14, focused on the development of materials and systems for the photoelectrochemical (PEC) production of hydrogen [2]. In Korea, the inception in 2003 of the 21st Century Frontier R&D Program by the Hydrogen R&D Research Center brought together a relatively broad range of topics to address challenges with a long term global view. Using a PEC composed of a TiO_2 single crystal as photoanode and Pt as cathode involving a chemical bias imposed by pH difference between the electrodes, Fujishima and Honda claimed a total efficiency of solar energy conversion to hydrogen of only 0.4%. Thereafter, many researchers have searched for other oxide materials that do not require external bias and exhibit higher light conversion, with TiO_2 and TiO_2-based materials being identified as the most promising candidates for photoanode [3]. Hence, a different approach using a photobiocatalytic system, rather than the development of new or modified photo-active materials, has been proposed. The photobiocatalytic method is a relatively novel way of producing hydrogen by coupling an inorganic semiconductor with an enzyme. This approach, with the enzyme being the main consideration, has been studied by many researchers since the mid 80's. However, the present study was performed from the photocatalytic point of view in combination with the electrochemical setups. The system naturally uses the intrinsic proton reduction ability of hydrogenase enzyme in tandem with an anodic compartment where the electron donors undergo light irradiation.

In *in-vitro* biological systems for hydrogen production, complex electron transport systems exist such as photosystem (PS) II and I, and ferredoxin (FD). These electron transport systems can theoretically be easily replaced with a photocatalyst or visible-light sensitized photocatalyst. Thus, the photocatalyst sensitized by light irradiation produces electrons and holes (electron vacancies), which can then be separated to reduce protons and oxidize the electron donor. For the photocatalyst particles to be activated by visible light, nitrogen-substituted TiO_2 (TiON) has been studied, either by sputtering or by hydrolyzing an aqueous $Ti(SO_4)_2$ solution with a NH_3 solution [4,5]. Moreover, the efficiency of the charge separation is not related to absorption of the light with the wavelength shorter than that of the bandgap energy, but depends rather on the physical properties of the samples, such as the shape, distribution pores, crystalline phase and crystallinity, and the preparation and the post-deposition treatments, even though they must be considered simultaneously with the substrate. Hence, the effect of these physical properties needs to be considered. In addition, although the enzyme that was used from *Pyrococcus furiosus* (Pfu), which was first isolated by Bryant and Adams [6], is known to be remarkably resistant to inactivation by temperature and chemical agents, Pfu was deactivated

†To whom correspondence should be addressed.
E-mail: hkjoo@kier.re.kr

by irradiated light and oxygen and different pH and temperature were required. For this reason, a photobiocatalytic and PEC approach with a separated reaction part has been performed. Factorial design is recognized as a methodology for applying statistics to experimentation to see how responses (output variables) change and interact at different variable settings. Using this versatile tool, especially fractional factorial design (FFD), economizes on time and expense. Therefore, this method has occasionally been applied in the case of many variables which needed to be screened according to the level of significance.

EXPERIMENTAL

1. Sample Preparation

Visible light-activated, nitrogen-substituted titanium oxide ('TiON') was simply prepared by two methods: sol-gel and hydrothermal. P25 TiO_2 (Degussa, FRG), UV100 (Hombikat, FRG) and NT22 TiO_2 (NANO Co., Ltd. Korea) were used as raw materials and reference when necessary. For hydrothermal TiON ('HT-TiON'), anatase TiO_2 powders were placed into a teflon-lined autoclave with a 50 ml capacity. The autoclave was then filled with an aqueous solution of NaOH, at various molar concentrations up to 80% of the total volume of the autoclave, and was maintained under the desirable conditions without shaking or stirring during the heating process. Washing and drying were then performed. To narrow the conditions a one-third FFD experiment involving nine factor-level combinations (FLC) was used to reduce the size of the experiment. In a full factorial experiment, an FLC of 3^3=27 occurs when there are three factors and three levels for each factor. The selected factors consist of three levels of each NaOH concentration (1, 3 and 5 M), temperature (175, 220 and 225 °C) and time (12, 24 and 36 hr). As a preliminary experiment, raw TiO_2 for TiON was prepared by using titanium tetraisopropoxide (TTIP), isopropyl alcohol (IPA), acetic acid and water for comparison. Finally, nitrogen was substituted into HT-TiON by mixing TiO_2 powder with a NH_3 solution followed by drying. Low temperature TiON ('LT-TiON') was prepared using low temperature synthesis with triethylamine (TEA), resulting in anatase crystallite phase and a surface area of ca. 170 m^2/g.

Purified hydrogenase (*Pyrococcus furiosus*, Pfu) was purchased from Prof. Adams at the University of Georgia. Pfu activity remained stable for at least 48 hr after removal from the freezer. The activity assay of Pfu (21,834 unit/ml) was much higher than that of Clostridium butyricum (1,442 unit/ml) and Thiocapsa roseopersicina (1,704 unit/ml), as determined with Tris-HCl (50 mM, pH 8.5, 50 °C, absorbance at 570 nm). The specific activity (unit/mg, Bio-rad protein assay, absorbance at 750 nm) of Pfu was two to three times higher than that of the latter hydrogenases. The activity was lower in phosphate, but similar in EPPS buffer. Methyl viologen (MV), tris(hydroxymethyl)aminomethane (Tris), phosphate, MES, sodium formate, and sodium dithionite (Na-D) were obtained from Sigma and used as received.

PEC experiment was conducted in a two-compartment (anodic and cathodic elements connected via a Nafion membrane or salt bridge) reactor eventually, but was started in each separate compartment separately. The anodic compartment had a volume of 60 ml and was a cylindrical-shaped cell. Photocatalyst films were prepared by casting the photocatalyst sol mixed with polyethylene glycol (PEG from Fluka, MW 20,000) as a binder onto an indium-tin oxide (ITO) conducting substrate, and subsequent heat treatment at 450 °C for 30 min under air (ca. 10 mg coated in 1×1 cm^2). The cyclovoltammogram and photovoltage measurements were performed with a potentiostat (EG&G, Model 273A) with an SUS316 electrode and Ag/AgCl (saturated in KCl) as a counter and reference electrode, respectively, in the anodic compartment containing an aqueous solution of 0.1 M Na_2S and 0.02 M Na_2SO_3. Cathodic experiments were performed in a water-jacketed, cylindrical-shaped cell with EPPS (50 mM, pH 8) buffer sealed with a silicone rubber gasket.

2. Apparatus and Analysis

The light sources used were UV-A lamp (Sankyo Denki, Japan), halogen lamp, xenon lamp (Oriel, USA, 1000W output max. with water filter) and LED (green and blue peaked at 520 nm and 464 nm, respectively). IPA was used as a probe compound for measuring the activity. The chemicals (IPA, acetone and CO_2) were analyzed by gas chromatography with a flame ionization detector (GC/FID, HP 5890) and a GC/FID with a methanizer (HP6890). Hydrogen production was analyzed by gas chromatograph with TCD (thermal conductivity detector at 160 °C). The column used in the system was molecular sieve 5A. Typical oven temperature was maintained at 40 °C. A moisture trap (silica-gel) was placed just before the GC auto injection valve to prevent water damage. The structure, morphology and surface area were investigated by using X-ray diffraction (XRD, Rigaku, DMAX/2000-Ultima Plus), scanning election microscopy (SEM, Topcon SM-720), and Brunauer Emmett Teller (BET).

RESULTS AND DISCUSSION

Initially, a rough hydrothermal experiment with NH_4OH and the prepared raw TiO_2 (189 m^2/g) revealed that the sample turned yellow and absorbed light with wavelength<ca. 520 nm. In addition, using aqueous NaOH (10 M) and a 12 hr reaction time under reaction temperatures ranging at 25 °C intervals from 100-200 °C, five samples exhibited the beta phase TiO_2 (β-TiO_2; Na_2TiO_3, $Na_2Ti_3O_7$) from XRD analysis with a maximum specific surface area of 246 m^2/g at 175 °C. The addition of silica led the particle size to conform to a more uniform distribution (a fibrous shape was identified by SEM [7]). The following properties, specific surface area, pore radius and pore volume, were changed with respect to the washing procedure used, showing a linear relationship between the specific surface area and pore radius. This suggests that the action of washing and its procedure are essential for removing impurities and controlling the shape.

The photo-active TiO_2 was systematically prepared by using FFD, a tool for experimental setup [8]. From analysis of the variance (ANOVA), the reaction temperature had 99% level of significance on the specific surface area. The NaOH concentration was critical to the phase formed. The anatase phase was formed with 1 M of NaOH, the β phase with 5 M of NaOH, and for 3 M of NaOH the anatase phase was formed below 225 °C and β phase above 225 °C. The specific surface area increased from 65 m^2/g to 144 m^2/g for 5 M NaOH, at 225 °C and 12 hr. A fibrous shape of TiO_2 was revealed at NaOH concentrations >3 M. Detailed investigations based

Table 1. Physical properties of samples from selected FLCs

	P25	NT22	4M200T12 (8/2w)SiO2	4M200T12	3M225T36	5M225T12
Phase	anatase+rutile	anatase	anatase	anatase	anatase+β-TiO_2	β-TiO_2
XRD intensity (θ)	545 (25.18)	1392 (25.16)	688 (25.30)	528 (25.26)	454 (25.26)	262 (24.26)
1/2 width	0.36	0.42	0.43	0.43	0.46	-
BET (m^2/g)	50	64.7	127.6	102.7	52.3	144.0
Pore vol. (cm^3/g)	-	0.228	0.448	0.365	0.189	0.566

on 3 M NaOH, at 175 °C and 12 hr were examined in terms of the phase and shape, by firstly varying the NaOH concentration (3.5, 4, 4.5 M) and subsequently varying the reaction temperature and time. The resulting optimum condition was found to be 4 M of NaOH, at 200 °C and 12 hr (103 m^2/g). A summary of the physical properties of the selected samples is given in Table 1, and their photocatalytic activity in degrading IPA using UV-A irradiation was investigated where P25 showed the fastest reaction rate, followed by NT22. The optimized sample (4M200T12-8/2w) showed a better activity than the other samples prepared, but was less active than the two commercialized TiO_2 samples under UV-A irradiation. The observed change in surface area was attributable to the crystallization of walls separating mesopores, as the loss in surface area increased the pore diameter and decreased the pore volume [9]. The optimized sample (4M200T12-8/2w) was further analyzed by DSC to identify the heat-treatment temperature to substitute nitrogen, where a distinguishable exothermic band appeared near 430 °C. This exothermic reaction was attributed to be the oxidation reaction of NH_3 or NH_2 with the oxygen released from the amorphous grain boundaries by forming oxygen-deficient sites [5]. This band was not significant due to the small amount of the amorphous portion in the samples obtained by the hydrothermal method, a result which needs to be further studied in terms of the ease and extent of nitrogen-substitution. As a consequence, NH_3 treatment, followed by heat-treatment at 450 °C, produced yellow powders (HT-TiON). A commercially available, blue LED (with a peak at 464 nm) was used to check the photocatalytic activity of the obtained HT-TiON. Acetone evolution as a function of blue LED irradiation time was remarkable for the HT-TiON sample, but no acetone was detected for the NT22 sample (P25 also revealed no acetone production in another study by the authors; data not shown).

To obtain direct insight for photo/biocatalytic hydrogen production system, two sets of one-third FFD experiments involving 9 FLC were used in order to reduce the size of the experiment: a full FFD experiment with FLC of 3^3=27. The factors included species of buffer solution, the amount of hydrogenase (Pfu), electron donor, reaction temperature and electron mediator. The correlation between electron mediator and Pfu was also studied by one half of 2^4 designs (8 FLCs). For a fixed hydrogenase (Pfu), four factors ($CdCl_2$, Na-dithionite, sodium formate and MV) were tested in terms of presence (two levels) in a designed manner. The ANOVA results showed that the amount of Pfu and Pfu+species of buffer was significant at the 0.25 significance level for the H_2 production. Moreover, Pfu+pH of Tris was significant at the 0.1 significance level and each of factors A and B was significant at the 0.025 significance level for the H_2 production. The two-factor interactions showed significant effect on the response variables. The described photo/biocatalytic system has been proposed as a possible candidate for hydrogen production technique with solar irradiation. Rough photonic efficiency was calculated according to the following two Eqs. (1) & (2).

$$\phi = \frac{K_{H_2}}{K_{irr}} \tag{1}$$

where K_{H_2} denotes the amount of produced H_2 in mol/s and K_{irr} the irradiated light in mol (photon)/s.

$$K_{irr} = \int \frac{1}{U_\lambda} d\lambda = \int \frac{I \times \lambda}{hcN_A} d\lambda \tag{2}$$

Here, I represents the measured light intensity [W], h Planck's constant, c the speed of light in vacuum, N_A Avogadro's number, and λ the representative wavelength of irradiated light [386 nm]. The measured total intensity I of ca. 700 μW/cm^2 (in the range of 310-386 nm when using a halogen lamp) was about one-fifth of the solar UV irradiation on earth (3-4 mW/cm^2). The calculated K_{irr} was 20.3×10^{-10} mol photon/s. According to a reference, solar irradiation is 1.5×10^{-6} mol/s per 1.4245×10^{-2} m^2 [10], equating to 105×10^{-10} mol photon/s per cm^2. This is also five times higher than the measured intensity I. As a result, with 20 mg of photocatalyst approximately 5.6×10^{-10} mol H_2/s was produced, giving a rough photonic efficiency of close to 30%. This value was reasonably valid given that the intensity of the irradiated light was low and the highest H_2 evolution rate with the photo/biocatalytic system was 30×10^3 μmol/(hr·g) [11], which is a few hundred times higher than that with typical TiO_2-based photocatalytic systems (several hundred μmol/(hr·g)). Fig. 1 shows a schematic view of the summarized reaction mechanism of the mixed slurry system where electron movement from the photocatalyst to the relay chemical was identified as the rate determining step. As a preliminary result, the following two factors were selected for consideration toward the next progress. First, was the separation of the photocatalyst and hydrogenase to overcome barriers such as instability of hydrogenase to photon and back reaction of hydrogen to water; and second, from the system's point of view, was either immobilization of the photocatalyst and hydrogenase or connection of both materials via an electron relay, which consequently prevents deactivation and enhances durability.

A two-compartment reactor was fabricated to optimize the photo/biocatalytic hydrogen production. Before experiments for hydrogen production were conducted, photoanodic and cathodic compartments were studied individually. When a semiconductor is in contact with an electrolyte, two areas are brought together: the solid-state physics and the electrochemistry. A connection between these two systems must be made to describe the PEC system. This is accomplished since the Fermi level in the semiconductor and the redox potential of the electrolyte are actually the same electrochemi-

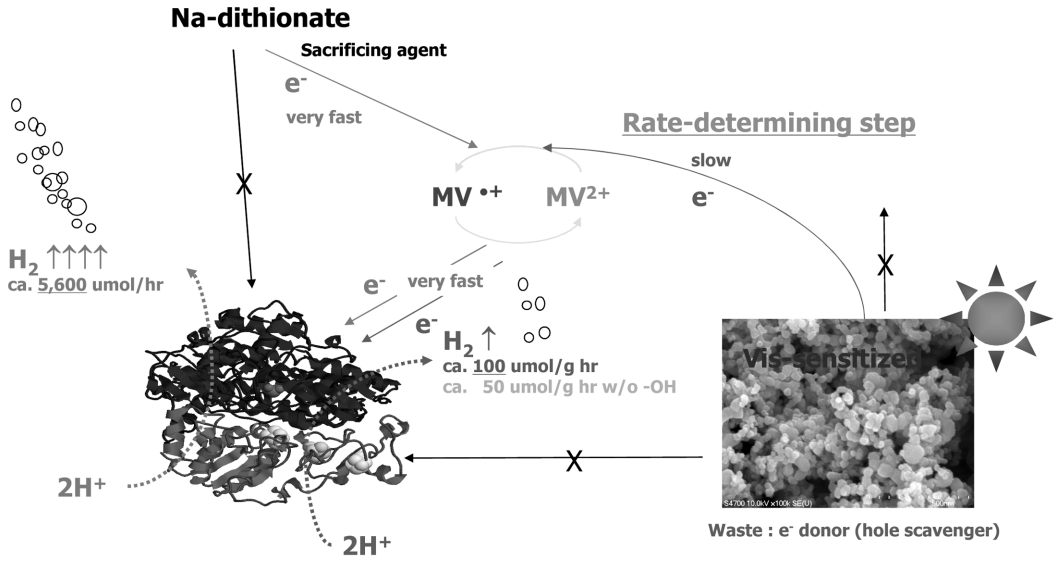

Fig. 1. Schematic view of the mechanism for the photo/biocatalytic hydrogen production system.

cal potential of the electron. The junction formed between an n-type semiconductor and an electrolyte when they are in contact brings about the band bending via charge transfer, and the excess charge is distributed in a space charge region. The extent of the band bending is a few tenths of a volt for a ca. 50 nm in diameter semiconductor [12,13].

In the case of the photoanode, nitrogen-substituted TiO_2 (TiON) powder was prepared and pasted on the conducting oxide. Then, with this photoanodic cell, the time coursed voltage curves (V-t, V_{oc} @ I=0), an important criterion of PEC performance characteristics, and cyclovoltammograms (I-V curves) were drawn to obtain useful electrochemical values. V_{oc} is the electromotive force of the cell which defines the maximum possible voltage across the cell in light when no current is flowing. It also represents the energy difference between the Fermi level of a semiconductor film and the reduction couple in the solution. During the light-off period, the cell exhibited a voltage of ca. −0.3 V and imposition of light increased the photo-voltage to the level of −1.0 V and of −0.7~−0.8 V without and with 400 nm cutoff filter, respectively. This photo-voltage is higher than that previously described in the literature [14,15]. It is also interesting to note that the voltage drop during the light-off period was substantially slower (2-3 hr) than voltage increase during the light-on period (20-60 min). This result is similar to that of from Bak et al., which they postulated was due to polarization-related phenomena. In the meantime, TiON300 and TiON400 exhibited a remarkable aspect in V-t analysis where the potential drop in the presence of 400 nm-cutoff filter was not as big as that with TiON450 or P25 TiO_2, indicating that TiON300 and TiON400 were efficient in producing charge carriers by light in the visible range. Both TiON300 and TiON400 also revealed the highest activity for photocatalytic IPA degradation with blue LED. The aforementioned band bending can be zero at the potential, called the flatband potential (E_{fb}), where no excess charge exists (no electric field and no space charge region). This flatband potential is important as it gives the approximate position of the conduction band of an n-doped semiconductor. E_{fb} can be determined by Butler's equation [16] as follows. By

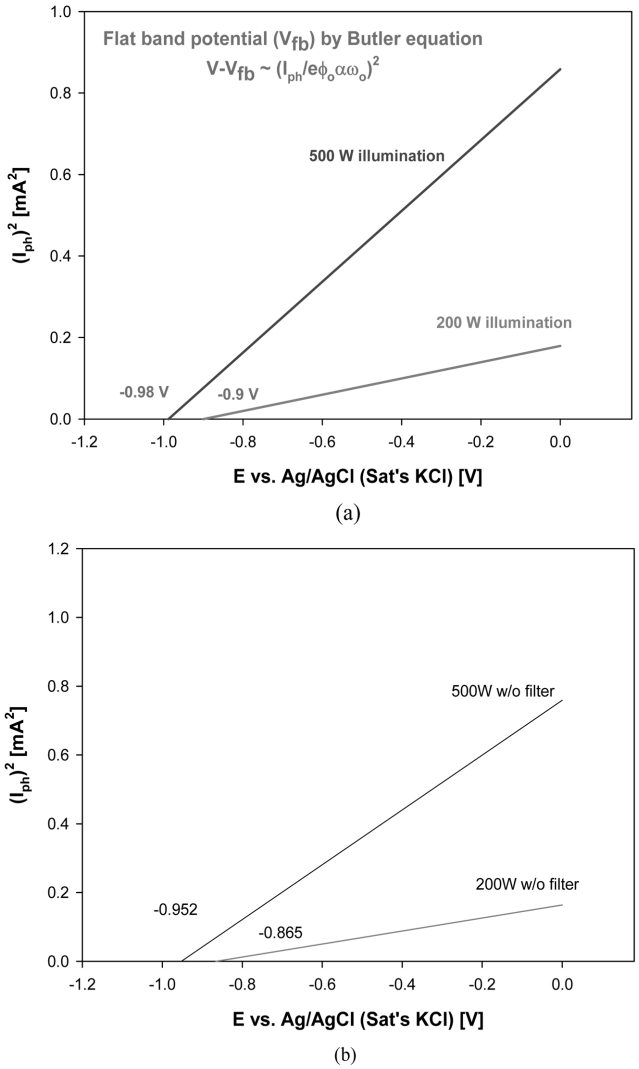

Fig. 2. $(I_{ph})^2$ vs. V plots for P25 (top) and TiON450 (bottom) for V_{fb} determination.

plotting V vs. I_{ph}^2, it is possible to determine E_{fb} when I_{ph}^2 is zero (Eq. (3)).

$$V - E_{fb} \approx (I_{ph}/e\phi_o \alpha \varpi_o)^2 \quad (3)$$

When illuminated, the band edges and Fermi level of an n-type semiconductor shift to more negative potential and the amount of band bending reduces. Our results showed that E_{fb} for prepared TiONs was in the range of −0.7~−0.8 V vs. SHE (Fig. 2), which indicates that an unbiased system can theoretically produce hydrogen at pH= 9 where $E^+_{H/H2}$ is −0.53 V vs. SHE [15]. In Fig. 3 the change in the hydrogen production rate is shown with respect to applied external bias and the amount of injected chemicals for EPPS buffer in the cathode compartment. External bias (critical bias seems to be 0.5 V) was found to be more important that the amount of chemicals in terms of hydrogen production rate.

Finally, the combination of obtained results produced a postulated energetic scheme for the photo/biocatalytic hydrogen production system (Figs. 4 & 5). Generally speaking, if the anodic current starts to flow at a potential considerably more negative than the cathodic current on the counter electrode, this implies that the driving force for the anodic current is enhanced by photovoltage indicative of an n-type semiconductor and the related reaction occurs in a cell spontaneously with no external bias. As shown in Fig. 5 where the internal bias already exists resulting from the pH difference of the electrolytes, the negative shift of the Fermi level of photo-anode leads to a higher driving force and more negative energetic level for electron transfer to the cathode and proton reduction.

Subsequent addition of Pfu and MV into the cathodic compartment while the anodic compartment was illuminated dramatically changed the trend of H_2 evolution, as shown in Fig. 6 (top). The simultaneous injection of Pfu and MV at the beginning of the reaction also produced a similar curve shape to that of the last part of the subsequent case (Fig. 6, bottom). MV only seldom produced H_2, while Pfu only did produce a little H_2 but much less than with-

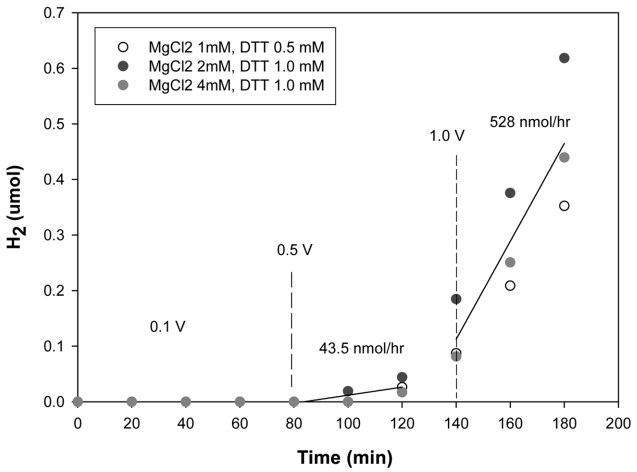

Fig. 3. Effect of external bias and injected chemicals in the cathodic compartment on the hydrogen production rate.

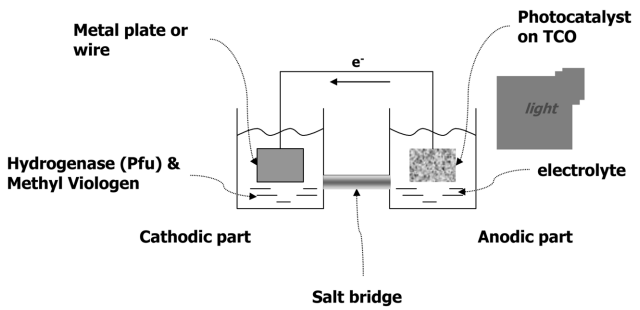

Fig. 4. Schematic view of the photobiocatalytic hydrogen production system.

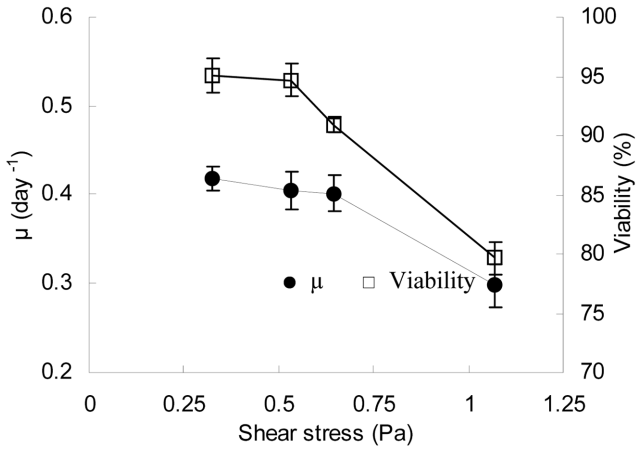

Fig. 5. Energetic view of redox potentials of components for the photobiocatalytic hydrogen production system.

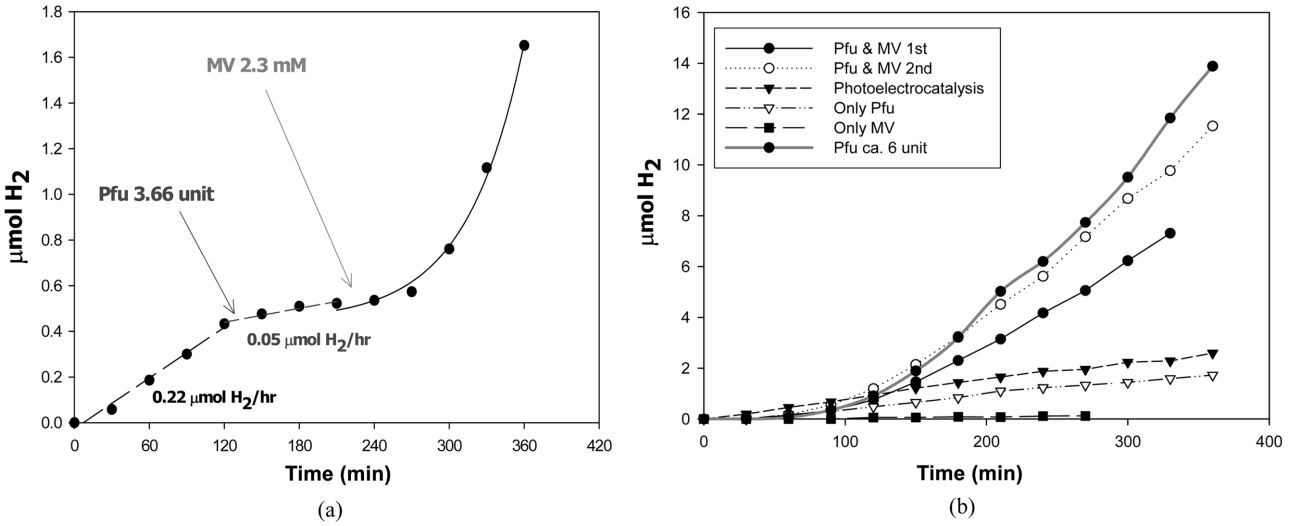

Fig. 6. Trend of hydrogen production according to the order of additive injection.

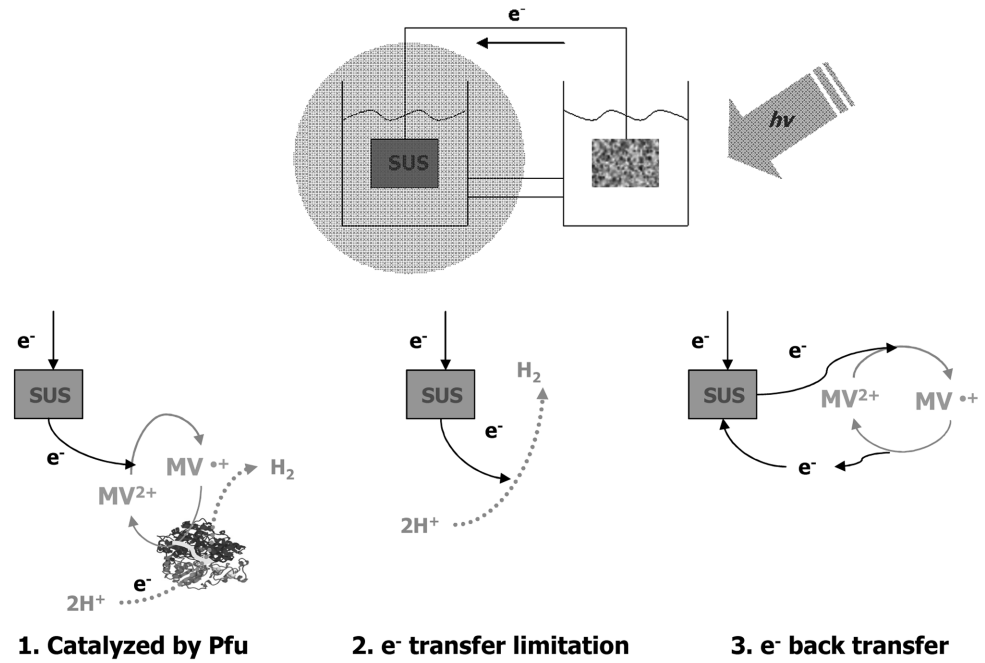

Fig. 7. Suggested explanation for three different reaction conditions (1: with MV and Pfu, 2: without MV and Pfu, and 3: with MV only).

out it. The absence of any direct electron transfer between conductor and enzyme was observed by Gurunathan [17]. The possible reason for those phenomena is illustrated in Fig. 7 where the back transfer of electrons in $MV^{+\bullet}$ to the metal cathode was detrimental in proton reduction, whereas the co-existence of MV and biocatalyst (Pfu) eased the transfer of electrons to protons. As expected, reaction medium for the biocatalyst drastically affected the rate of H_2 production (Fig. 8), which might be caused partly from the internal bias due to pH difference intrinsically, but partly from characteristics of buffers considered with a fixed pH. Since the buffer played a role as an electron donor in the photobiocatalytic system, the hydrogenase species and buffer may be related.

CONCLUSIONS

For hydrogen production with solar irradiation, a relatively novel approach was described where sensitized photocatalysts donate electrons to hydrogenase that in turn reduces protons into hydrogen. Since the subtle effect of the morphology of the photocatalyst and microstructure in photocatalysis did not seem to be critical in the photobiocatalytic hydrogen production system, the requirements for the development of the photocatalyst were reduced, which increases the feasibility of the solar-driven system for future hydrogen production. Individual photoanodic and cathodic experiments demonstrated the close energetic relation of the system, while simultaneous PEC experiments also produced promising results with evidence of an exponential trend in hydrogen production. As well as improving the stability of the system, research attention is now focusing on increasing the rate to an economical level.

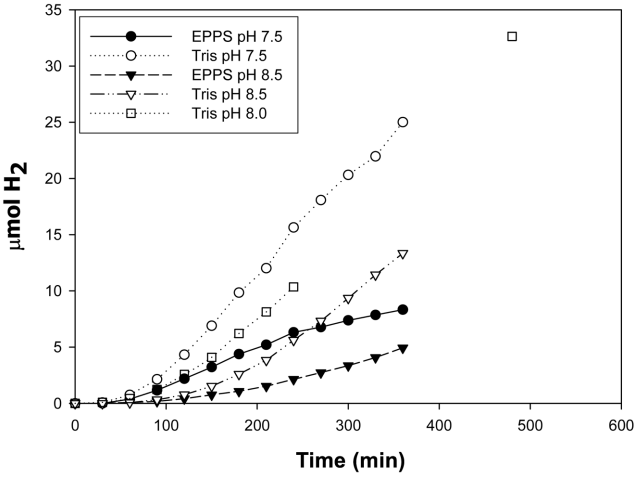

Fig. 8. Effect of buffer on photobiocatalytic hydrogen production.

ACKNOWLEDGMENTS

This research was performed for the Hydrogen Energy R&D Center, one of the 21st Century Frontier R&D Programs, funded by the Ministry of Science and Technology of Korea.

REFERENCES

1. G. B. Raupp, A. Alexiadis, M. Hossain and R. Changrani, *Catalysis Today*, **69**, 41 (2001).
2. A. Luzzi, *Final report for IEA Hydrogen Program Annex-14* (2004).
3. T. Bak, J. Nowotny, M. Rekas and C. C. Sorrell, *Int. J. Hydrogen Energy*, **27**(1), 19 (2002).
4. R. Ashai, T. Morikawa, T. Ohwaki, K, Aoki and Y. Taga, *Science*, **293**, 269 (2001).
5. T. Ihara, M. Miyoshi, Y. Iriyama, O. Matsumoto and S. Sugihara, *Applied Catalysis B: Environmental*, **42**(4), 403 (2003).
6. F. O. Bryant and M. W. W. Adams, *J. Biol. Chem.*, **264**(9), 5070 (1989).
7. W. Wang, O. K. Varghese, M. Paulose, C. A. Grimes, Q. Wang and E. C. Dickey, *J. Mater. Res.*, **19**(2), 420 (2004).
8. D. C. Montgomery, *Design and analysis of experiments*, John Wiley & Sons, USA (1991).
9. T. Sreethawong, Y. Suzuki and S. Yoshikawa, *J. Solid. State Chem.*, **178**(1), 329 (2005).
10. D. Ljubas, *Energy*, **30**(10), 1699 (2005).
11. P. Pedroni, G. M. Mura, G. Galli, C. Pratesi, L. Serbolisca and G. Grandi, *Int. J. Hydrogen Energy*, **21**(10), 853 (1996).
12. M. Larsson, MS thesis in Lund University, Sweden (2001).
13. R. Memming, *Semiconductor electrochemistry*, Wiley-VCH, Weinheim, FRG (2001).
14. C. He, X. Li, Y. Xiong, X. Zhu and S. Liu, *Chemosphere*, **58**(4), 381 (2005).
15. L. G. Arriaga and A. M. Fernández, *Int. J. Hydrogen Energy*, **27**(1), 27 (2002).
16. M. A. Butler, *J. Appl. Phys.*, **48**(5), 1914 (1977).
17. K. Gurunathan, *J. Molecular Catalysis A: Chemical*, **156**, 59 (2000).